

# Initial results from the field testing of the “rotor as a sensor” concept

M. Bertelè and C.L. Bottasso

Wind Energy Institute, Technische Universität München, Garching bei München, Germany

E-mail: [marta.bertele,carlo.bottasso@tum.de](mailto:marta.bertele,carlo.bottasso@tum.de)

**Abstract.** This work reports preliminary findings on the field validation of the “rotor as a sensor” concept. In a nutshell, the idea is to use the rotor response in order to measure the wind inflow, effectively turning the whole rotor into a sort of generalized anemometer capable of estimating wind speed, shears and directions. In turn, these quantities can be used for optimizing turbine and farm-level performance. Here a purely data-driven method is used, where a wind observer is first identified using flow field measurements (obtained by a met-mast) together with the corresponding blade root load harmonics. Once the observer has been identified, the wind inflow is estimated online during turbine operation by feeding it with measured blade root harmonics. Preliminary results reported herein seem to be very encouraging.

## 1. Introduction

Reliable and accurate information on the wind inflow can be of significant help when it comes to improving the performance of a single wind turbine as well as of a whole wind farm. For example, having a precise knowledge of the rotor pointing direction with respect to the wind can allow for an improved machine alignment and, in turn, for increased power harvesting and decreased fatigue loads. Similarly, information about the horizontal shear can be exploited for wake detection in cooperative control strategies, whereas a correct estimate of the vertical shear can help quantify the stability of the atmosphere, which deeply influences wake behaviour. Other uses of the inflow at the rotor disk are possible and, indeed, turning each turbine into a sophisticated wind sensor can provide a wealth of opportunities for smart operation, monitoring and prediction.

Standard nacelle-mounted sensors are commonly used to measure the wind inflow. Apart from their not always straightforward calibration, they provide only pointwise (as opposed to rotor-equivalent) measurements, and hence cannot measure spatially varying wind characteristics such as shears. LiDARs overcome such limitations, but are not yet in widespread use and are still mostly confined to research applications or special uses.

A novel methodology was proposed by the authors (see [1, 3] and references therein), which has the ambition to overcome such problems. First, a map is created that links the wind inflow with the turbine response. Once the map has been generated, it is used to estimate the wind inflow during turbine operation by using measurements of the rotor response in terms of loads. For machines already equipped with such sensors (for example, for load reduction control), the implementation of the “rotor as a sensor” concept can be regarded as a simple software upgrade. The method was characterized with extensive numerical tests [7, 1, 2] and using scaled models



operated in a boundary layer wind tunnel [3]. A previous version of the formulation was also tested using data obtained on the CART3 experimental turbine at NREL [5]. In this work, we report a more extensive test campaign performed on a multi-MW wind turbine, aimed at better characterizing the performance of this new wind sensing technology and at indicating directions for its future improvement.

The paper is structured as follows: the mathematical formulation of the wind observer and its identification procedure are presented in section 2, while a preliminary analysis of its field performance can be found in section 3. Finally, section 4 concludes the paper and provides an outlook on future work.

## 2. Formulation

### 2.1. Wind parametrization

Following [1, 3], the wind inflow is parametrized by two directions and two shears (cfr. Fig. 1): the upflow  $\chi$  and yaw  $\phi$  angles, and the vertical  $\kappa_v$  and horizontal  $\kappa_h$  linear shears. For notational convenience, such parameters are grouped together in the wind state vector as follows:

$$\boldsymbol{\theta} = \{\phi \ \kappa_v \ \chi \ \kappa_h\}^T. \quad (1)$$

The sheared wind inflow is described as

$$W(y, z) = V_h \left( \frac{z}{z_h} \kappa_v + \frac{y}{R} \kappa_h \right), \quad (2)$$

where  $V_h$  and  $z_h$  are the wind speed and the vertical coordinate at hub height, respectively, while  $R$  is the rotor radius. It follows that the three wind speed components in the nacelle-attached frame of Fig. 1 can be expressed as

$$u(y, z) = W(y, z) \cos \phi \cos \chi, \quad (3a)$$

$$v(y, z) = W(y, z) \sin \phi \cos \chi, \quad (3b)$$

$$w(y, z) = W(y, z) \sin \chi. \quad (3c)$$

### 2.2. Wind observer formulation

The wind observer is based on a map between wind inflow and machine response. More specifically, steady wind conditions characterized by the four wind states generate a periodic response of the wind turbine. Following the analysis of Ref. [1], the wind state vector is linearly related to the one per revolution (1P) harmonics of the blade root bending moments as follows

$$\mathbf{m} = \mathbf{F}(V)\boldsymbol{\theta} + \mathbf{m}_0(V) = [\mathbf{F}(V) \ \mathbf{m}_0(V)] \begin{bmatrix} \boldsymbol{\theta} \\ 1 \end{bmatrix} = \mathbf{T}(V) \bar{\boldsymbol{\theta}}, \quad (4)$$

where  $\mathbf{F}$  and  $\mathbf{m}_0$  represent the model coefficients, scheduled with respect to the wind speed  $V$ . The machine response is represented by vector  $\mathbf{m}$

$$\mathbf{m} = \{m_{1c}^{\text{OP}}, m_{1s}^{\text{OP}}, m_{1c}^{\text{IP}}, m_{1s}^{\text{IP}}\}^T, \quad (5)$$

which groups the blade root in-plane and out-of plane bending moments, respectively noted  $m^{\text{IP}}$  and  $m^{\text{OP}}$ , with subscripts  $(\cdot)_{1s}$  and  $(\cdot)_{1c}$  indicating 1P sine and cosine harmonics.

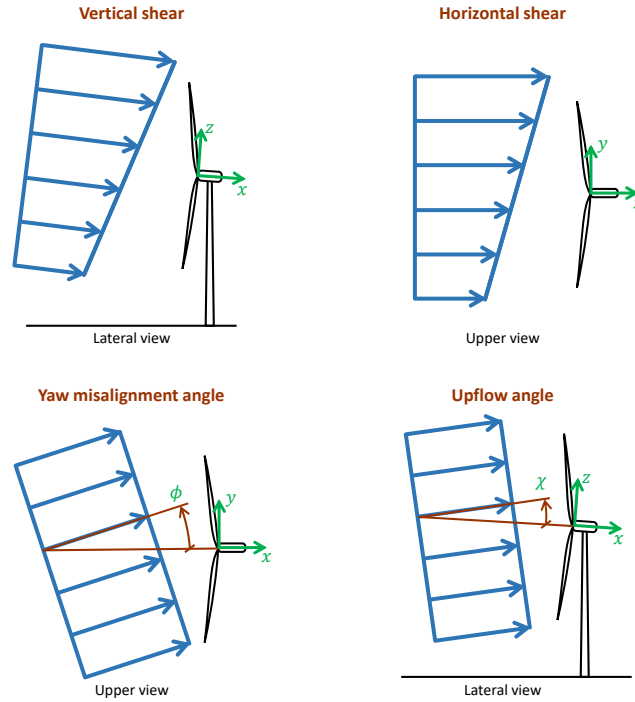


**Figure 1.** Wind state parameters characterizing the inflow at the rotor disk.

### 2.3. Wind observer identification

In order to identify the model expressed by Eq. (4), i.e. compute the coefficients  $\mathbf{F}$  and  $\mathbf{m}_0$ , a rich enough dataset of known blade measurements  $\mathbf{M} = \{\mathbf{m}_1, \dots, \mathbf{m}_N\}$  is collected along with the corresponding known wind inflows  $\Theta = \{\theta_1, \dots, \theta_N\}$ , which gives

$$\mathbf{M} = \mathbf{T}\Theta. \quad (6)$$

Inverting the system, one obtains

$$\mathbf{T} = \mathbf{M}\Theta^T(\Theta\Theta^T)^{-1}. \quad (7)$$

The post-processing of the dataset and the calculation of the model coefficients is performed off-line, and it takes of the order of a few minutes on a standard desktop PC.

Once the model coefficients are known, the wind state estimates  $\theta_E$  can be observed by using the following expression

$$\theta_E = (\mathbf{F}(V)^T \mathbf{R}^{-1} \mathbf{F}(V))^{-1} \mathbf{F}(V)^T \mathbf{R}^{-1} (\mathbf{m}_M - \mathbf{m}_0), \quad (8)$$

where  $\mathbf{m}_M$  are given measured loads and  $\mathbf{R}$  is the co-variance weighting matrix. The estimation of the wind states is performed on-line during wind turbine operation, and it has a negligible computational cost.

The identification procedure can be simplified by the method proposed in Ref. [3], which exploits the rotational symmetry of the rotor to reduce the unknown coefficient in matrix  $\mathbf{F}$ .

This leads to the following identities

$$F_{i1} = \frac{\partial m_{1c}}{\partial \phi} = -\frac{\partial m_{1s}}{\partial \chi} = -F_{j3}, \quad (9a)$$

$$F_{j1} = \frac{\partial m_{1s}}{\partial \phi} = \frac{\partial m_{1c}}{\partial \chi} = F_{i3}, \quad (9b)$$

$$F_{i2} = \frac{\partial m_{1c}}{\partial \kappa_v} = \frac{\partial m_{1s}}{\partial \kappa_h} = F_{j4}, \quad (9c)$$

$$F_{j2} = \frac{\partial m_{1s}}{\partial \kappa_v} = -\frac{\partial m_{1c}}{\partial \kappa_h} = -F_{i4}, \quad (9d)$$

where  $i = 1$  and  $j = 2$  for the out-of-plane components, while  $i = 3$  and  $j = 4$  for the in-plane ones. This way, the unknown coefficients are reduced from 16 to 8 and, most importantly, independent variations within the identification dataset of only two of the four wind parameters are necessary, namely one angle and one shear.

### 3. Results

In this work, field measurements were used to first identify and then evaluate the performance of the wind observer. SCADA data recorded at 10Hz on a 3.5MW eno114 machine provided the necessary operational data. Wind conditions were measured by a met-mast reaching to hub height (92 m) and placed 2.5 diameters (D) away from the turbine. The blade moments were measured by strain gauges placed at the root of the blades. To extract the 1P harmonics of in and out-of plane loads, the Coleman transformation [9] was used along with an appropriate low pass filter.

#### 3.1. Wind parametrization in the field

The hub-height wind direction measured by the met-mast was first filtered with a moving average and then shifted in time to account for the delay induced by the distance between met-mast and wind turbine.

The met-mast is equipped with two anemometers, one located at hub height and one at the lower point of the rotor disk. This is indeed a rather typical situation, which follows the standard certification guidelines [10]. To compute a vertical shear over the whole disk vertical height, the method of Refs. [6, 8] was used. This approach uses the blades as local wind sensors; averaging over a desired azimuthal angle, it yields an estimate of the wind speed over sectors of the rotor disk. Four sectors were used in this work, resulting in the top, bottom, left and right quadrants. From these four values, one can derive estimates of both the vertical and horizontal shears over the whole rotor. On the other hand, discarding the top quadrant, one can derive an estimate of the vertical shear up to hub height, which can be directly correlated with the measurements provided by the met-mast. Figure 2 shows a clear correlation between 10 minute averages of the vertical shear extrapolated from the met-mast and the one computed with the observer of Ref. [6].

Finally, the rotor-effective wind speed was computed from the torque-balance equation [4, 11, 12]. The rotor-effective wind speed is used as scheduling parameter of the wind estimator, whose coefficients are assumed to vary as functions of the turbine operating condition.

#### 3.2. Wind observer performance

The model was identified by using the measured wind shears and horizontal wind direction. The effects caused by the upflow angle, which was not directly known from the met-mast data, was on the other hand reconstructed by using the symmetry conditions expressed by Eqs. (9a) and (9b).

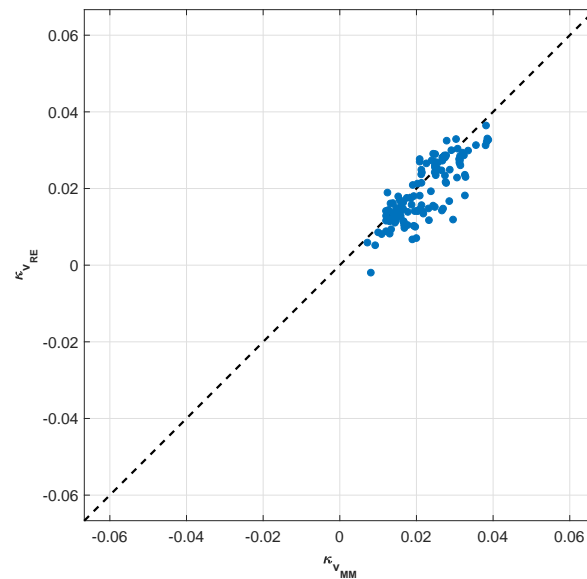


**Figure 2.** Correlation between 10 minute averages of the met-mast extrapolated ( $x$ -axis) and observed ( $y$ -axis) shears.

In the following, the performance of an observer identified from data collected during one day of operation (14.11.2017) is presented. The identification dataset was cleaned from non-operative conditions and excessive turbulence levels, while retaining a sufficiently wide range of wind speeds (from 5 to 12  $\text{ms}^{-1}$ ) and inflow variations. As a result, about 20% of the data collected on that day was used for identification, whilst another 70% was used for validation. Figure 3 shows the performance of the observer for each parameter over time: the black markers represent the reference quantities — derived as explained in §3.1, which therefore can hardly be considered as an exact ground truth — while the blue and red markers indicate the observer estimation over the validation and identification sets, respectively.

It appears that the wind shears are estimated very well, with a slight decrease in accuracy in the second part of the day, i.e. with increasing levels of turbulence intensity (TI). Slightly higher errors can be observed in the yaw misalignment estimate, which nevertheless appears to follow quite accurately the reference. No specific claim can be made for the upflow angle, as the reference is unknown. Nonetheless, it should be noted that the mean value of the upflow angle does not vary significantly, which is indeed what can be expected in the present case, given the flatness of the surrounding terrain.

To further test the robustness of the observer, the same model was used to estimate the wind parameters measured on a different day (specifically, on 24.11.2017). Figure 4 shows the estimation results over time. Here again, the results indicate a notable accuracy in the instantaneous estimates of both vertical and horizontal shears, as well as a good overall accuracy in the mean wind direction.

The significant degradation of the estimates between 11 am and 3 pm is due to very low wind speeds (lower than 5  $\text{ms}^{-1}$ ), which lie below the velocity range covered by the model identification. These points should therefore not be considered for judging the quality of the results, but only indicate the danger of extrapolating and the importance of using an

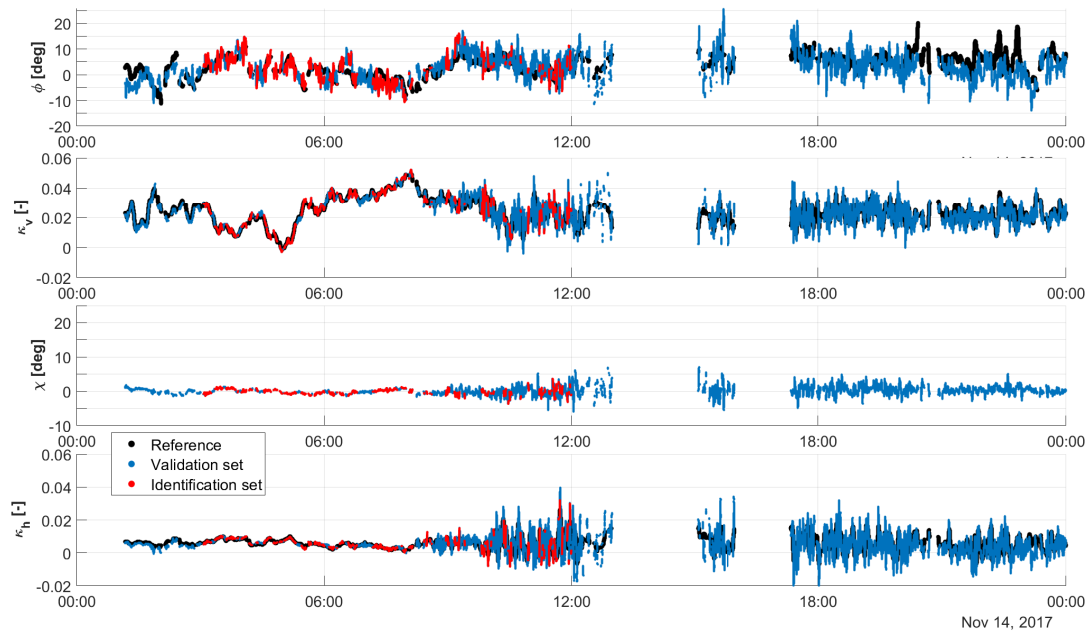


**Figure 3.** Time histories of the four wind states on 14.11.2017. Black: reference; red: identification set (i.e. data points used for model identification); blue: validation (i.e. observations of data points not used for identification).

identification dataset that covers the whole range of speeds of interest.

Finally, to obtain a more complete picture of the observer performance over these two days, Fig. 5 shows 10 minute averages of the estimated parameters (reported on the  $y$ -axis) with respect to the reference ones (reported on the  $x$ -axis), binned over wind speed. The correlation is in general very good. A few points show a significant scatter, but they only correspond to low wind speeds that were not included in the identified model. The estimates appear very accurate as far as the shears are concerned, while the wind direction is affected by somewhat larger errors. Overall, such results confirm the trends already noted in Refs. [1, 3].

#### 4. Conclusions

In this paper, the methodology described in Refs. [1, 3] was applied to field data collected on a 3.5 MW wind turbine. The present dataset is quite interesting, because it represent the typical setup that can normally be expected for the certification of a wind turbine, the wind inflow being measured with a hub-height met-mast.

Results indicate not only the feasibility of the proposed methodology, but also promising results. In fact, the wind parameter estimates follow very well both the vertical and horizontal shears. The horizontal wind direction is slightly less accurate, although its main trends are still captured quite well.

The work is continuing on two main fronts. On the one hand, a more extensive dataset is being analyzed to consider the effects of atmospheric parameters such as TI and density on the overall observer performance. On the other hand, measurements obtained by a scanning LiDAR during the same measurement campaign are being processed, in order to compare the estimates to yet another reference.

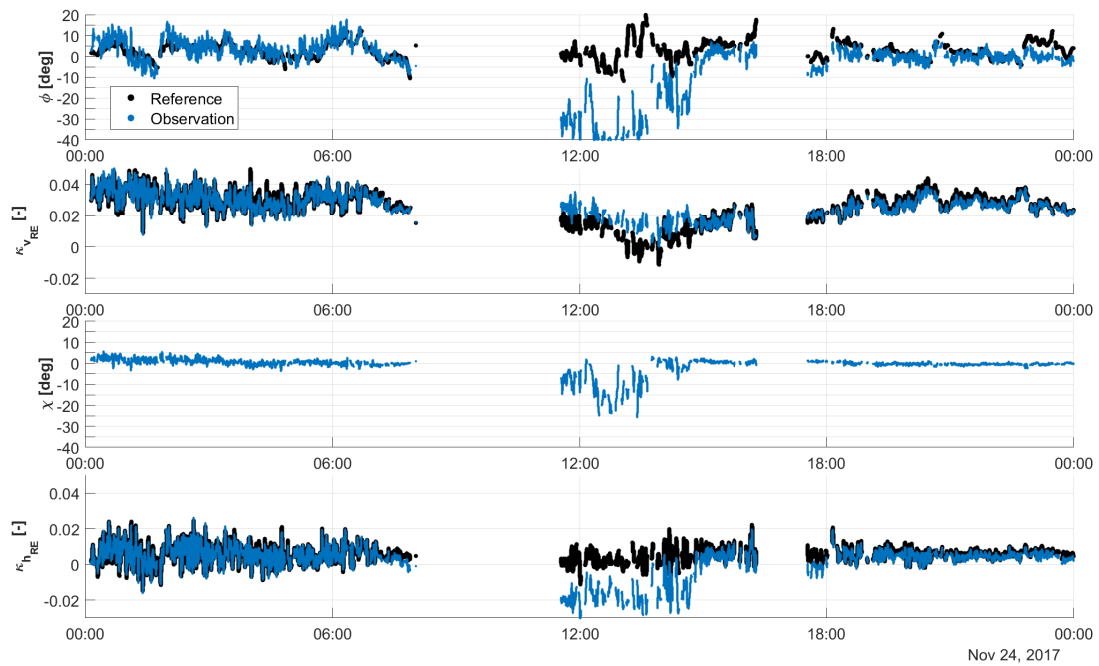


**Figure 4.** Time histories of the four wind states on 24.11.2017, using the model identified on 14.11.2017. Black: reference; blue: observation.

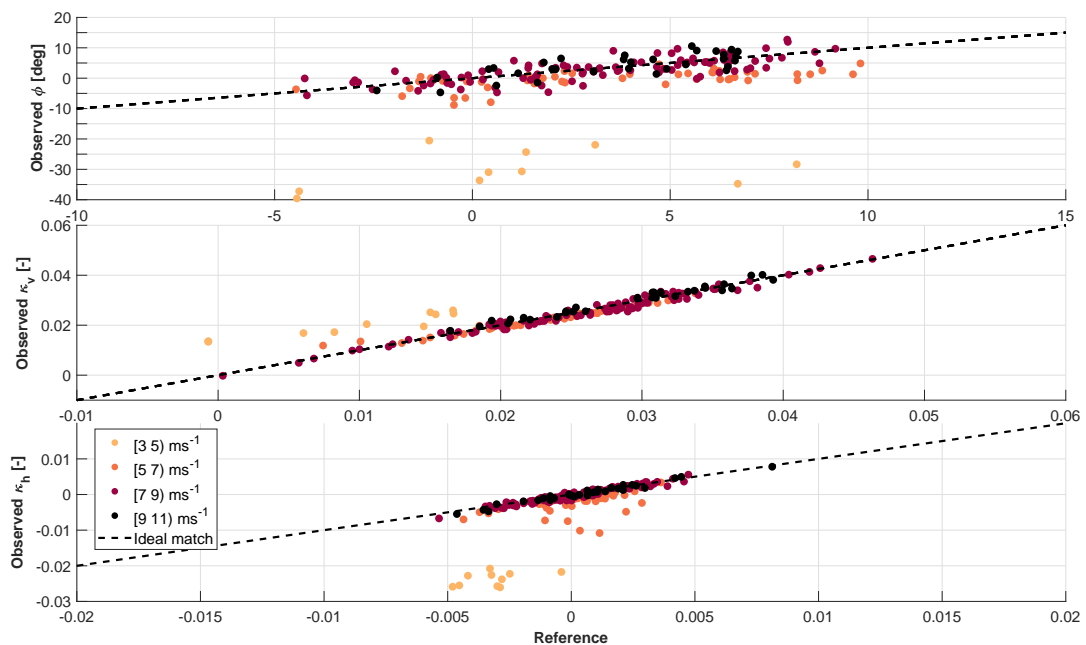


**Figure 5.** Correlation between 10 minute averages of the observed ( $y$ -axes) wind parameters and their reference values ( $x$ -axis) for different wind speed bins.

### Acknowledgments

The authors wish to acknowledge for their support eno energy systems GmbH and the Compact Wind 2 Project, the latter receiving founding from the German Federal Ministry for Economic

Affairs and Energy (BMW).)

## References

- [1] Bertelè M, Bottasso CL, Cacciola S, Daher Adegas F, and Delpont S 2017 Wind inflow observation from load harmonics. *Wind Energ. Sci.*, <https://doi.org/10.5194/wes-2017-23>.
- [2] Bertelè M, Bottasso CL and Cacciola S 2018 Simultaneous estimation of wind shears and misalignments from rotor loads: formulation for IPC-controlled wind turbines. *J. Phys. Conf. Ser.*, 1037.
- [3] Bertelè M, Bottasso CL and Cacciola S 2019 Brief communication: Wind inflow observation from load harmonics wind tunnel validation of the rotationally symmetric formulation. *Wind Energ. Sci.*, 4, 89-97, <https://doi.org/10.5194/wes-4-89-2019>.
- [4] Bottasso CL and Croce A 2009 Advanced Control Laws for Variable-speed Wind Turbines and Supporting Enabling Technologies. *Technical Report*, Dipartimento di Ingegneria Aerospaziale, Politecnico di Milano.
- [5] Bottasso CL and Riboldi CED 2015 Validation of a wind misalignment observer using field test data. *Renew. Energy* 74 298–306.
- [6] Bottasso CL, Cacciola S and Schreiber J 2018 Local wind speed estimation, with application to wake impingement detection. *Renewable Energy* 116, 155168, [dx.doi.org/10.1016/j.renene.2017.09.044](https://doi.org/10.1016/j.renene.2017.09.044).
- [7] Cacciola S, Bertelè M, Bottasso CL 2016 Simultaneous observation of wind shears and misalignments from rotor loads. *J. Phys. Conf. Ser.*, 753.
- [8] Campagnolo F, Schreiber J, Garcia AM and Bottasso CL 2017 Wind Tunnel Validation of a Wind Observer for Wind Farm Control *International Society of Offshore and Polar Engineers*, ISOPE-I-17-410, <https://www.onepetro.org/conference-paper/ISOPE-I-17-410>
- [9] Coleman RP and Feingold AM 1958 Theory of self-excited mechanical oscillations of helicopter rotors with hinged blades. *Technical Report*, NACA TN 1351.
- [10] International Electrotechnical Commission 2013 CDV IEC 61400-12-1. *Technical Report*, International Electrotechnical Commission, Geneva, Switzerland.
- [11] Ma X, Poulsen N and Bindner H 1995 Estimation of Wind Speed in Connection to a Wind Turbine. *Technical Report*, Informatics and Mathematical Modelling, Technical University of Denmark.
- [12] Soltani M, Knudsen T, Svenstrup M, Wisniewski R, Brath P, Ortega R and Johnson K 2013 Estimation of rotor effective wind speed: a comparison. *IEEE Trans. Control Syst. Technol.* 21 (4) 1155e1167, <https://doi.org/10.1109/tcst.2013.2260751>.